Ceramics International **24** (1998) 35–43

PII: S0272-8842(96)00074-0
0272-8842/97 $17.00+.00

Effect of Cubic Phase on the Kinetics of the Isothermal Tetragonal to Monoclinic Transformation in ZrO_2(3 mol% Y_2O_3) Ceramics

W. Z. Zhu*

Institute for Nonmetallic Materials, Swiss Federal Institute of Technology (ETH), CH-8092, Zurich, Switzerland

(Received 12 December 1995; accepted 23 July 1996)

Abstract: In this paper, the effect of cubic phase on the kinetics of the isothermal tetragonal (t) to monoclinic (m) transformation in ZrO_2(3 mol% Y_2O_3) ceramics was studied by means of thermal expansion analysis (TEA), scanning electron microscopy (SEM), transmission electron microscopy (TEM) and X-ray diffractometry (XRD). Experimental results showed that the kinetics of the isothermal t→m transformation could be expressed using the Johson–Mehl–Avrami equation, i.e.

$$f = 1 - \exp(-kt^n)$$

where f refers to the volume fraction of transformed m-phase, k is a variable associated with the energy barrier for critical nucleation and growth, and n is a constant depending on the nucleation sites. It was found that both the "nose" temperature and the incubation periods of the TTT curve of the ZrO_2(3 mol% Y_2O_3) ceramics were decreased in comparison with those of the TTT curve of the ZrO_2(2 mol% Y_2O_3) ceramics. The time–temperature–transformation (TTT) curve is C-shaped, with the "nose" temperature determined to be 300°C. Activation energy for transformation was regressed to be 22·74 kJ/mol, which didn't change with temperature. TEM observation revealed that preferential growth of cubic phase grains refined t-phase grains during hot-pressing. It is proposed that the nucleation and longitudinal growth of m-phase plates in ZrO_2(Y_2O_3) ceramics are displacive, while the sidewise growth thereafter is controlled by short-range diffusion of oxygen ions and, in this sense, the t→m transformation in ZrO_2(Y_2O_3) ceramics possesses both displacive and non-displacive features. © 1997 Elsevier Science Limited and Techna S.r.l.

1 INTRODUCTION

Transformation toughening through the tetragonal (t) to monoclinic (m) transformation in ZrO_2 alloys is believed to be one of the most effective ways of improving the toughness and reliability of structural ceramics. Although our knowledge of this aspect has advanced considerably, e.g. it is generally agreed that control of the metastability of the t-phase is the key to obtaining optimum toughening effect and is affected by such factors as content of stabilizer, grain size, shape and site of the t-phase grains, as well as constraints imposed by the neighbouring matrix,[1–3] many problems still remain unsolved. The stress-triggered t→m transition occurring in ZrO_2 alloys is usually considered to be athermal, but may also show some isothermal character.[4–7] This isothermal component of the transformation has received relatively little attention. There are divided views on the nature of the kinetics of the isothermal t→m transformation in ZrO_2(Y_2O_3) ceramics. Results by Nakanishi and Shigematsu[8] have shown that the kinetics of the isothermal t→m transformation is controlled by the diffusion of oxygen ions with the implication of

*Present address: Department of Materials Science and Engineering, Zhejiang University, Hangzhou 310027, P. R. China.

bainite transformation, which is quite different from results of their previous studies.[9] Heuer *et al.*[10] pointed out that the t→m transformation in 3Y–TZP ceramics displays both athermal and isothermal kinetics; they are both stress-assisted martensitic transformations. They viewed the athermal character usually found in a cooling transformation as due to rapid isothermal transformation of the most easily nucleated regions at a succession of temperatures. In other words, a range of activation energies exists for such martensitic transformations. Up to now, no experimental data has been obtained to confirm this deduction. The intent of the present paper is to interpret the character of the kinetics of the t→m transformation in ZrO_2(3 mol% Y_2O_3) ceramics, which consist of cubic, tetragonal and monoclinic phases, and to propose an appropriate mechanism.

2 EXPERIMENTAL PROCEDURES

Powders of zirconia containing 2 mol% and 3 mol% yttria in solid solution, respectively, with purity higher than 99% and average diameter of about 0·1 μm, were cold-pressed into pellets of 24 mm×6 mm×6 mm in size under a pressure of 300 MPa, followed by pressureless sintering at 1600°C with 5 h holding time. A relative density of more than 98% could be obtained. Thermal expansion analysis experiments were performed on a Perkin–Elmer 7 Series Thermal Analysis System with polished specimens, machined to be 4 mm×4 mm×3 mm in size. The point at which a tangential line deviates from the thermal expansion curve was defined as the transformation temperature. The relative amount of monclinic phase was calculated using the formula proposed by Garvie,[11] according to the X-ray diffraction results:

$$M\% = \frac{I_m(11\bar{1}) + I_m(111)}{I_m(11\bar{1}) + I_m(111) + I_{ct}(111)}$$

where $I_m(11\bar{1})$ and $I_m(111)$ refer to the relative peak strengths of the $(11\bar{1})$ and (111) planes of the monoclinic phase, respectively, and $I_{ct}(111)$ represents the relative peak strength of the (111) plane of the tetragonal or cubic phase. A sample for TEM inspection was prepared by the conventional procedure of grinding, dimpling and ion-thinning to perforation, followed by coating with a thin film of amorphous carbon to avoid charging and JEM100 type microscopy was operated with 120 kV as the accelerating voltage.

3 RESULTS AND DISCUSSION

3.1 Thermal expansion curves of ZrO_2(2 mol% Y_2O_3) and ZrO_2(3 mol% Y_2O_3) specimens

Figure 1 shows the thermal expansion curves of ZrO_2(2 mol% Y_2O_3) and ZrO_2(3 mol% Y_2O_3) ceramics obtained at a heating and cooling rate of 10°C/min. Specimen size initially increases with increase in temperature, then drastically decreases as the temperature is increased above the A_s point (starting temperature of the m→t transformation), finally it increases again as the temperature is further increased above the A_f point (ending temperature of the m→t transformation). It is apparent that at temperatures above the A_f point, only t-phase exists in the specimen. Similarly, the specimen size initially decreases linearly with decrease in temperature until the M_s point (starting temperature of the t→m transformation), below which it increases significantly due to the dilatational nature of the t→m transformation. When the temperature is further decreased below the M_f point (ending temperature of the t→m transformation), thermal expansion curves reverse to the linear shrinkage section until ambient temperature. It should be noted that, in the present study, ZrO_2(2 mol% Y_2O_3) ceramics were sintered in the single t-phase region according to the phase

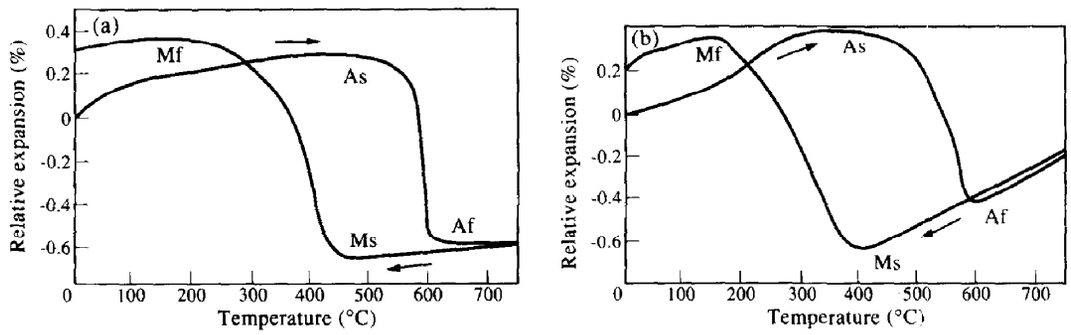

Fig. 1. Thermal expansion curves of $ZrO_2(Y_2O_3)$ ceramics obtained at a heating and cooling rate of 10°C/min: (a) ZrO_2(2 mol% Y_2O_3); (b) ZrO_2(3 mol% Y_2O_3).

Table 1. Starting and ending temperatures of the t→m and m→t transitions for ZrO_2(3 mol% Y_2O_3) and ZrO_2(2 mol% Y_2O_3) specimens sintered at 1600°C

Specimens	M_s	M_f	A_s	A_f
ZrO_2(3 mol% Y_2O_3)	387°C	142°C	374°C	542°C
ZrO_2(2 mol% Y_2O_3)	459°C	322°C	567°C	602°C

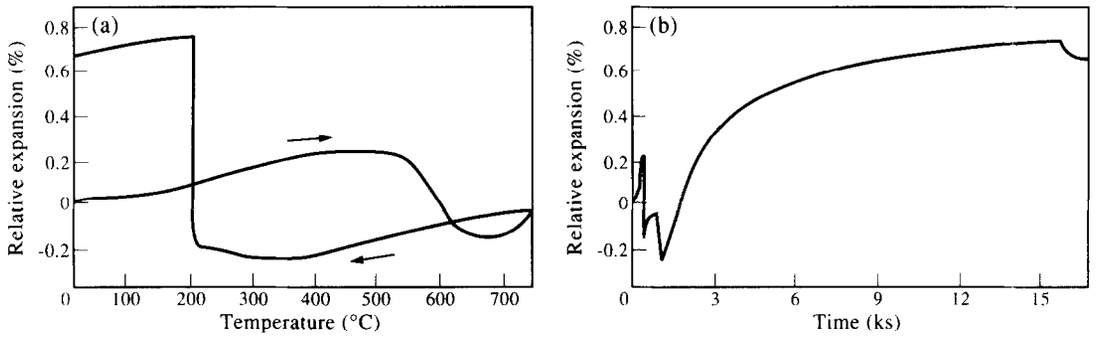

Fig. 2. Thermal expansion curves obtained at a heating and cooling rate 100°C/min for ZrO_2(3 mol% Y_2O_3) ceramics held at 200°C for 4 h: (a) curve of expansion vs temperature; (b) curve of expansion vs time.

Table 2. Results of thermal expansion and XRD measurements for ZrO_2(3 mol% Y_2O_3) specimens held at different temperatures for 4 h

Temperature (°C)	150	200	250	300	350
Pre-m phase	15.53%	13.4%	10.93%	13.23%	3.60%
Isothermal m-phase	16.40%	52.47%	49.68%	48.19%	15.70%
Athermal m-phase	0	0	2.69%	3.20%	7.20%
Overall m-phase	31.90%	65.80%	63.30%	64.40%	26.50%
Expansion before holding	0.3532%	0.2344%	0.1995%	0.24335%	0.2061%
Expansion during holding	1.0460%	0.9214%	0.9069%	0.8864%	0.4098%
Expansion after holding	0	0	0.04919%	0.0589%	0.4098%
Overall expansion	1.3990%	1.1510%	1.1510%	1.1880%	1.5120%

diagram.[12] The microstructure of the t+m dual phase obtained at room temperature implies that part of the sintered t-phase has transformed to m-phase during cooling. However, ZrO_2(3 mol% Y_2O_3) ceramics were sintered in the c+t dual phase region and the microstructure obtained at room temperature is composed of c, t and m-phases. Table 1 lists the transformation temperatures of ZrO_2(2 mol% Y_2O_3) and ZrO_2(3 mol% Y_2O_3) ceramics, which reveals that the appearance of c-phase results in the lowering of the transformation temperature.

3.2 Kinetics of the isothermal t→m transformation in ZrO_2(3 mol% Y_2O_3) ceramics

Thermal expansion curves obtained at a heating and cooling rate of 100°C/min for ZrO_2(3 mol% Y_2O_3) ceramics held at 200°C for 4 h are shown in Fig. 2: (a) refers to the curve of expansion vs temperature; (b) refers to the curve of expansion vs time. Results of thermal expansion and XRD measurements for specimens held at different temperatures for 4 h are listed in Table 2, from which it is evident that a cooling rate of 100°C/min is not high enough to inhibit the t→m transformation before holding, and the lower the holding temperature, the more pre-m phase produced prior to holding. Therefore, the initial phase constitutent for the measurement of the isothermal kinetics

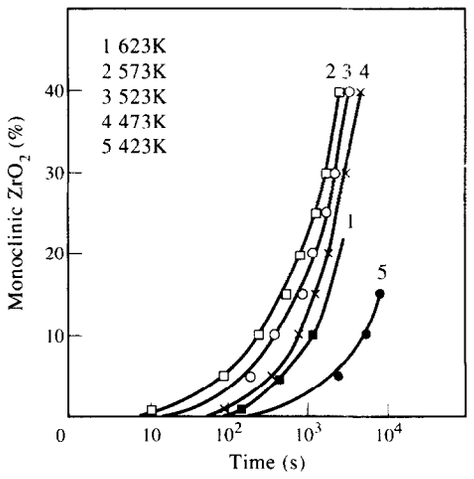

Fig. 3. Changes of the fraction of m-phase with holding time for ZrO_2(3 mol% Y_2O_3) specimens held at different temperatures for 4 h.

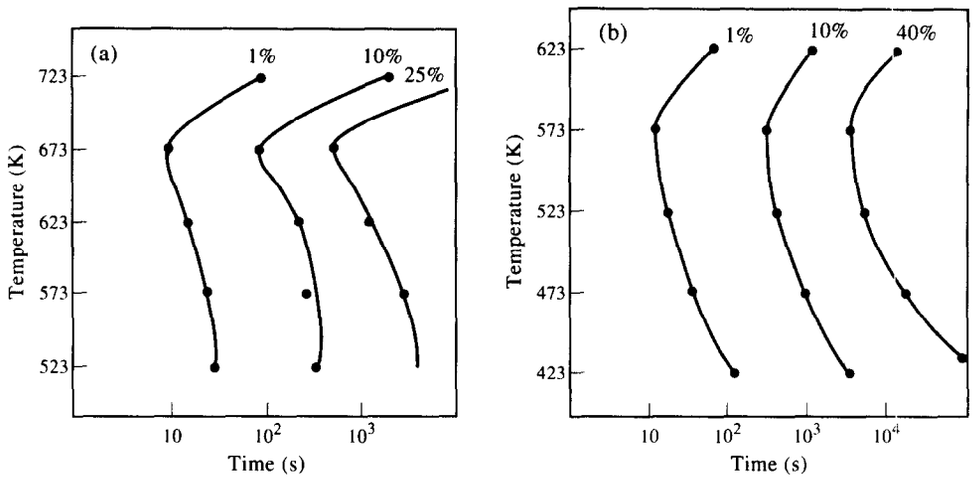

Fig. 4. Time–temperature–transformation (TTT) curves for the (a) ZrO_2(2 mol% Y_2O_3) and (b) ZrO_2(3 mol% Y_2O_3) specimens.

curve consists of t and m phases, and part of the t-phase transforms isothermally to m-phase during holding. Change of volume fraction of m-phase obtained during holding with time is shown in Fig. 3, and the corresponding time–temperature–transformation (TTT) curve turns out to be C-shaped with a "nose" temperature determined to be 300°C, as shown in Fig. 4. For comparison, the TTT curve of ZrO_2(2 mol% Y_2O_3) ceramics is also shown in Fig. 4. The kinetics of the isothermal t→m transformation possesses the following features:

(a) The existence of an incubation period which initially becomes shorter with a decrease in holding temperature, then becomes longer when the holding temperature is further decreased, resulting in the appearance of a "nose" temperature. The existence of an incubation period is one of the features of a diffusional transformation whose isothermal kinetics can be expressed in terms of the Johson–Mehl–Avrami (JMA) equation, i.e. $f = 1 - \exp(-kt^n)$, where f is the volume fraction of transformed phase, k is a variable associated with the energy barrier for critical nucleation and growth, and n is a constant depending on the nucleation sites. The TTT curve of ZrO_2(3 mol% Y_2O_3) ceramics lies to the down-left side of that of ZrO_2(2 mol% Y_2O_3) ceramics, indicating that at the same holding temperature, the incubation period of the former is shorter than that of the latter;

(b) The value of n, the exponent in the JMA equation, is somewhat different at different holding temperatures, implying slight variations of nucleating sites with holding temperature (Fig. 5).

(c) The functional relationship between $\ln(nk)$ and $1/T$, shown in Fig. 6, reveals the activation energy for the transformation to be 22·74 kJ/mol, irrespective of the holding temperature.

(d) The isothermal transformation cannot proceed to completion with part of the constrained t-phase remaining in the final microstructure.

As stated above, ZrO_2(3 mol% Y_2O_3) ceramics were fabricated in the c+t dual phase region at a sintering temperature of 1600°C, according to the binary ZrO_2–Y_2O_3 phase diagram.[12] Morphologies of the c-phase grains are comparatively easier to distinguish from those of the t-phase grains. It was previously reported that c-phase grains are relatively difficult to nucleate during sintering and once they nucleate, growing speed is much higher than that of t-phase grains until the phase equilibrium state, which can be ascribed to the fact that a small amount of c-phase grains are primarily located at

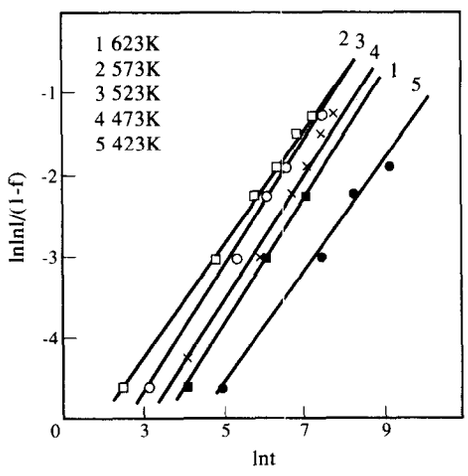

Fig. 5. Relationship between $\ln\ln 1/(1-f)$ and $\ln t$ for ZrO_2(3 mol% Y_2O_3) specimens.

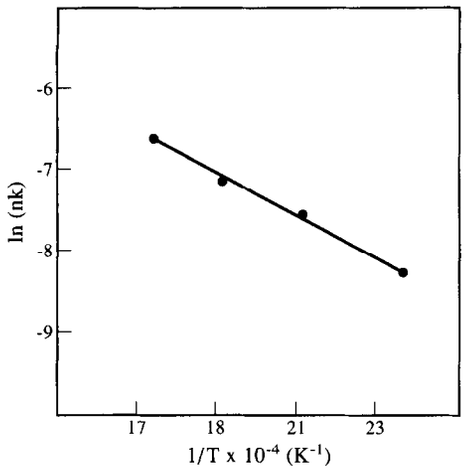

Fig. 6. Functional relationship between $\ln(nk)$ and $1/T$ for ZrO_2(3 mol% Y_2O_3) specimens.

the grain boundaries of the t-phase.[12] As a result, the size of c-phase grains is always larger than that of t-phase grains. SEM photographs of ZrO_2 (2 mol% Y_2O_3) and ZrO_2(3 mol% Y_2O_3) ceramics are simultaneously shown in Fig. 7, which indicates that the average grain size of t-phase in the former is larger than that in the latter with a small amount of larger c-phase grains. Therefore, in some sense, preferential growth of c-phase grains inhibits the growth of t-phase grains in ZrO_2(3 mol% Y_2O_3) ceramics and the existence of a small amount of c-phase grains refines the t-phase grains. The fact that the incubation periods of the TTT curves of ZrO_2(3 mol% Y_2O_3) ceramics are shorter than those of the TTT curves of ZrO_2(2 mol% Y_2O_3) ceramics can be attributed to the refinement of the t-phase grains through the existence of c-phase grains. The lower "nose" temperature of the TTT curve of ZrO_2(3 mol% Y_2O_3) ceramics as compared to that of ZrO_2(2 mol% Y_2O_3) ceramics can be explained by the lower starting temperature of the t→m transformation of ZrO_2(2 mol% Y_2O_3) ceramics. This is because the "nose" temperature of the TTT curve is largely determined by the starting temperature of the t→m transformation.

3.3 Microstructure of ZrO_2(3 mol% Y_2O_3) ceramics

Microstructure and morphologies of the m-phase are shown in Fig. 8, among which Fig. 8(a) indicates that the grain with dark contrast is monoclinic phase, while the grain with relatively bright contrast is t + m dual phase. Figure 8(b) shows the different morphologies of m-phase within two irregular t-phase grains. In one grain the m-phase takes the form of parallel laths, which is similar to the morphology of low-carbon martensite. Lath-shaped m-phase is one of the features of the microstructure in $ZrO_2(Y_2O_3)$ ceramics, which is different from those in pure zirconia. In another grain, the m-phase appears in the form of an "N" shape, large "N" typed m-phase passes across the grain and the un-transformed part of the grain is intercepted by a smaller one. "N" typed m-phase morphology is similar to that of high-carbon martensite. The different morphology of the m-phase is probably associated with different mechanisms of formation, in that "N" typed m-phase is indicative of auto-catalytic nucleation and coordinating growth and the whole process is much faster, while the formation of lath-shaped m-phase is relatively slower. Small triangular domains formed at intersections between lattice invariant shear (LIS) twins and deformation twins are shown in Fig. 8(c). It is significant that microcracks caused by collisions between the two kinds of twins appear at areas without triangular domains and vice versa, indicating that the triangular domain is essentially a type of coordinating twin, among which the LIS twin plane is $(001)_m$ and the twin plane of the triangular domain is $(011)_m$.[13] Figure 8(d) illustrates the case in which the m-plate is deflected by a

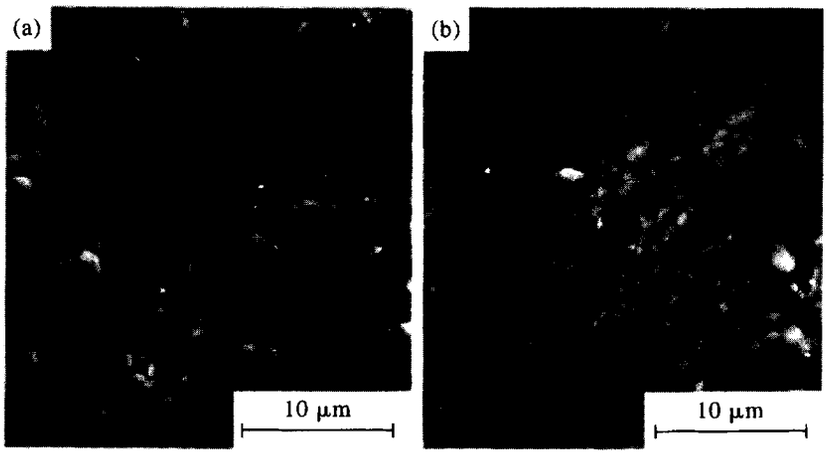

Fig. 7. SEM photographs showing the natural surfaces of (a) ZrO_2(2 mol% Y_2O_3) and (b) ZrO_2(3 mol% Y_2O_3) specimens.

dislocation during propagation, implying that the stress field of dislocation counteracts that of transformation.

Diffusional phase separation to produce precipitates of t-phase has obviously occurred within some regions of the c-phase grains during sintering, as shown in Fig. 9(a) and (b), respectively. Morphologies of the m-phase are quite different, in that "N" typed m-phase exists in Fig. 9(a) with microcracks at the grain boundary, while m-phase appears in the form of parallel laths in Fig. 9(b) without microcracks at the grain boundary. A diffraction pattern along the [111] direction is shown in Fig. 9(c), in which three (112) type forbidden spots appear. Figure 9(d) shows the dark field image taken by using a (112) forbidden spot, in which a "colony" microstructure — which is a characteristic of product of the c→t diffusional phase separation — is clearly observed. Every (112) reflection corresponds to one kind of "colony" variant, each of which is composed of two groups of twinned precipitating t-phase with planes determined to be $\{101\}_m$. It is found that regions with a lower yttria content in the c-phase grain are more favourable for the precipitation of t-phase, which can be accounted for as follows: (1) the lower the yttria content, the higher the equilibrium temperature between c and t phases, and the larger the effective driving force for precipitation; (2) nucleation of t-phase is kinetically favoured at regions with relatively low yttria content because the concentration of yttria is reduced in forming nuclei.

Comprehensively speaking, the phase constitutent in ZrO_2(3 mol% Y_2O_3) ceramics is rather complicated and is composed of cubic, tetragonal and monoclinic phases. The t-phase can be either sintered phase or precipitate depending on sintering temperature and cooling conditions. The grain size of the sintered t-phase is relatively small, while precipitates of t-phase are produced in the form of a "colony" microstructure through diffusional phase separation within large c-phase grains during high temperature sintering. The m-phase can either occupy the whole grain or co-exist with the t-phase within the original t-phase grains.

3.4 Mechanism of the isothermal t→m transition

In tetragonal ZrO_2, zirconium ions occupy sites of the face-centred tetragonal lattice, where the distribution of oxygen ions deviates slightly from the (001) plane, leading to the appearance of certain tetragonality. When Y_2O_3 is solid-solutioned into the ZrO_2 lattice, some of the zirconium ions are

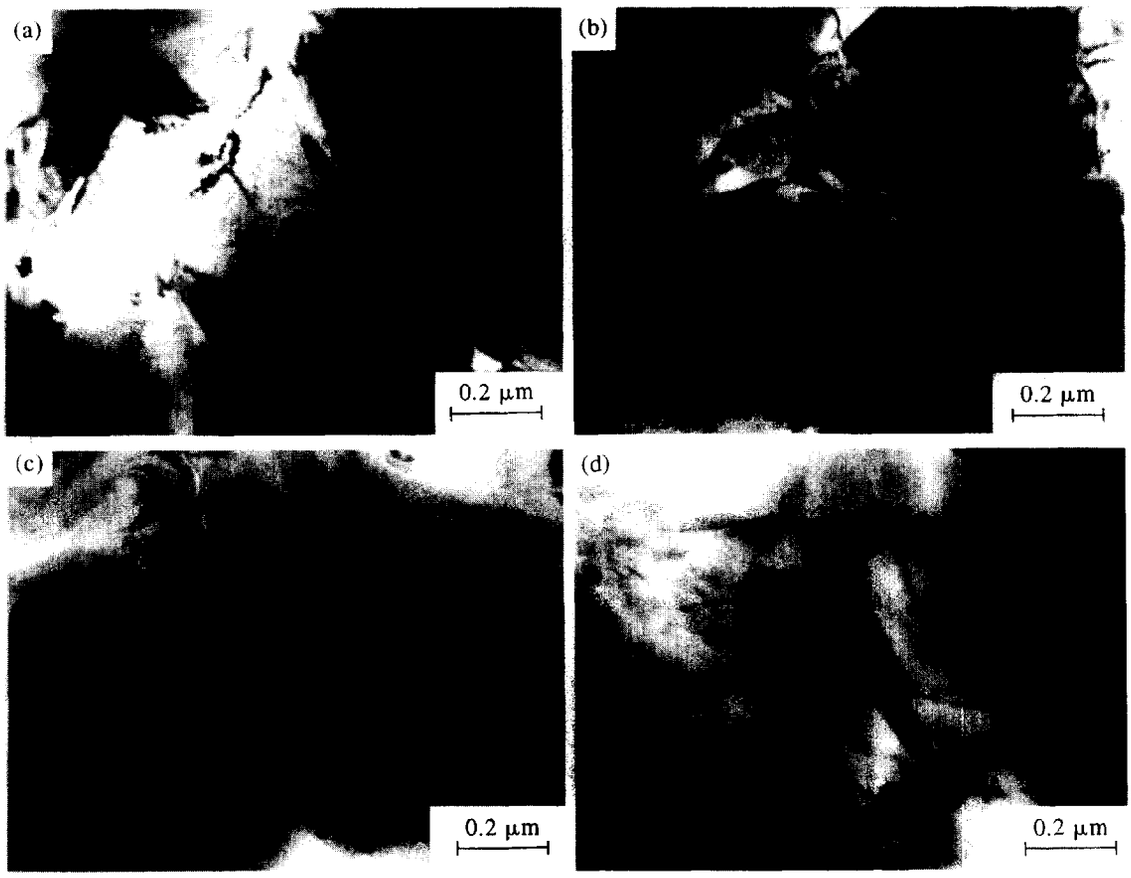

Fig. 8. TEM photographs showing the microstructure of ZrO_2(3 mol% Y_2O_3) specimens: (a) butterfly-like m-phase within a t-phase grain and distribution of yttria content within different grains; (b) morphologies of m-phase within different grains; (c) triangular domains in twinned m-phase; (d) interaction between the dislocations and the m-phase.

substituted for yttrium ions, during which a certain number of oxygen vacancies are expected to be produced to hold the ionic neutralization. The following reaction can be used to describe above process:[8]

$$ZrO_2 + Y_2O_3 \rightarrow 2Y_{Zr} + V_0 + 3O_0$$

where V_0 is the oxygen vacancy. The amount of oxygen vacancies can be characterized by following formula:[14]

$$V = \frac{4M}{100 + M}$$

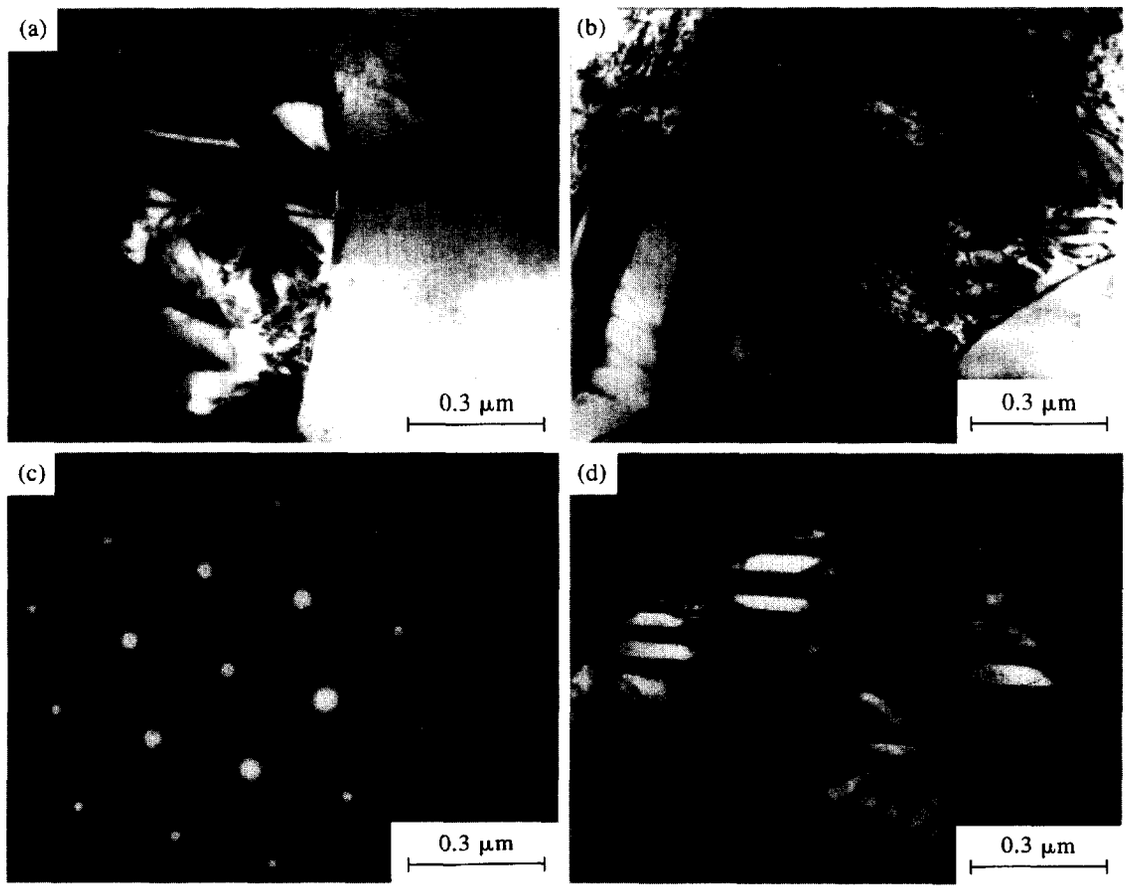

Fig. 9. Precipitation of t-phase within a c-phase grain of ZrO_2(3 mol% Y_2O_3) specimens: (a) and (b) bright field images showing the co-existence of c, t and m-phases; (c) diffraction pattern of the c-phase; (d) dark field image taken by using a (112) forbidden spot.

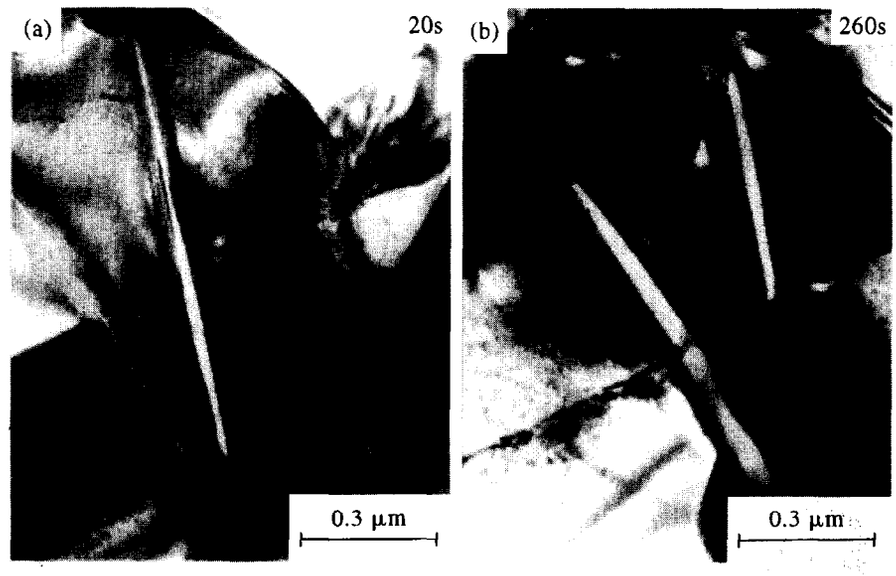

Fig. 10. TEM photographs showing the in-situ formation of parallel lathed m-phase, induced by the irradiation of an electron beam in a ZrO_2(2 mol% Y_2O_3) ceramic.

Here V is the volume fraction of oxygen vacancies and M is the concentration of Y_2O_3 in mol%. It can be seen that the concentration of oxygen vacancies increases with increasing Y_2O_3 concentration. Thus, it is proposed that in $ZrO_2(Y_2O_3)$ containing a large amount of vacancies, the transformation behaviour is quite different from that in pure zirconia.[15] For pure zirconia, when the t→m transformation occurs, the lattice composed of zirconium ions shears in a coordinating and military manner, concurrent with obvious volume expansion as well as shape change. As a result, this diffusionless shear process becomes a predominant factor in controlling the kinetics of transformation, which appears to be athermal. Because ceramic materials possess high strength and elastic modulus, the strain energy caused by a shear-like transformation is large and morpholgies of the final products, which are always twinned, are determined by the strain energy. For $ZrO_2(Y_2O_3)$ ceramics, when the t→m transformation occurs, not only a coordinating shift of zirconium ions is needed, but short-range diffusion of oxygen ions also takes place, with the implication that this kind of transformation possesses both displacive and non-displacive features. TEM photographs of the in-situ growth of m-phase induced by the irradiation of an electron beam are shown in Fig. 10, from which direct proof of heterogeneous nucleation of m-plates at the grain boundaries can be obtained. It is observed that the nucleation process is rather rapid and once nucleation completes, growth in the longitudinal direction is much faster than that in the tranverse direction. It is roughly estimated that the growing velocity along the longitudinal direction is 30 times faster than that along the tranverse direction. It is thus proposed that the nucleation and longitudinal growth of m-phase plates in $ZrO_2(Y_2O_3)$ ceramics is believed to be displacive, while the sidewise growth thereafter is proved to be short-range diffusion controlled. The short-range diffusion of oxygen ions becomes a predominant factor in controlling the kinetics of the t→m transformation in $ZrO_2(Y_2O_3)$ ceramics. The release of the large transformation strain incurred by the expansion of monoclinic phase through the short-range diffusion of oxygen ions might be responsible for the diversity of m-phase morphologies observed in $ZrO_2(Y_2O_3)$ ceramics. In view of the fact that the transformation activation energy calculated using the kinetics data is in the range of 20–40 kJ/mol, which is far less than the activation energy for self-diffusion of oxygen ions (96 kJ/mol),[16] it is speculated that the shifting distance of the oxygen ions during transition is less than the lattice constant of the tetragonal phase (0·50 nm).

4 CONCLUSIONS

(a) The time–temperature–transformation (TTT) curve for the t→m transformation in ZrO_2(3 mol% Y_2O_3) ceramics is C-shaped, with a "nose" temperature determined to be 300°C. The TTT curve of ZrO_2(3 mol% Y_2O_3) ceramics lies to the down-left side of that of ZrO_2(2 mol% Y_2O_3)ceramics.

(b) Preferential growth of c-phase grains in ZrO_2(3 mol% Y_2O_3) ceramics effectively refines the grain size of the t-phase.

(c) The microstructure of ZrO_2(3 mol% Y_2O_3) ceramics is very complicated, in that it contains tetragonal phase (which can either be a sintered phase or precipitates), monoclinic phase (which can either occupy the whole grain or co-exist with the tetragonal phase) and cubic phase.

(d) The mechanism of the t→m transition in $ZrO_2(Y_2O_3)$ ceramics is different from that in pure ZrO_2. The nucleation and longitudinal growth of m-phase plates in $ZrO_2(Y_2O_3)$ ceramics are displacive, while the sidewise growth thereafter is controlled by short-range diffusion of oxygen ions and, in this sense, the t→m transformation in $ZrO_2(Y_2O_3)$ ceramics possesses both displacive and non-displacive features.

REFERENCES

1. CHEN, I. W. & CHIAO, Y. H., *Acta Metall.*, **33**(10) (1985) 1827.
2. HEUER, A. H., CLAUSSEN, N., KRIVEN, W. M. & RUHLE, M., *J. Am. Ceram. Soc.*, **65**(12) (1982) 642.
3. SUBBARAO, E. C., *Advances in Ceramics, Science and Technology of Zirconia*, Vol. 3. American Ceramics Society, Columbus, OH, 1981, p. 1.
4. SATO, T., OHTEKI, S., ENDO, T. & SHIMADA, M., *J. Am. Ceram. Soc.*, **68**(10) (1985) C-320.
5. NAKANISHI, N. & SHIGEMATSU, T., *Mater. Trans. JIM*, **33**(3) (1992) 318.
6. LEI, T. C., ZHU, W. Z. & ZHOU, Y., *Mater. Chem. Phys.*, **34**(4) (1993) 317.
7. ZHU, W. Z., LEI, T. C. & ZHOU, Y., *J. Mater. Sci.*, **28**(12) (1993) 6479.
8. NAKANISHI, N. & SHIGEMATSU, T., *Mater. Trans. JIM*, **32**(8) (1991) 778.
9. NAKANISHI, N. & SHIGEMATSU, T., *Zirconia Ceram.*, **8**(1) (1986) 71.
10. BEHRENS, D., DRANSMANN, G. W. & HEUER, A. H., *J. Am. Ceram. Soc.*, **76**(4) (1993) 1025.
11. GARVIE, R. C., *J. Am. Ceram. Soc.*, **55**(6) (1972) 303.
12. RUHLE, M., CLAUSSEN, N. & HEUER, A. H., *Advances in Ceramics, Science and Technology of Zirconia II*, Vol. 12. American Ceramics Society, Columbus, OH, 1984, pp. 352.
13. WOLTEN, G. M., *J. Am. Ceram. Soc.*, **46**(10) (1963) 418.
14. INGEL, R. P. & III, D. L., *J. Am. Ceram. Soc.*, **69**(4) (1986) 325.

15. BANSAL, G. K. & HEUER, A. H., *Acta Metall.*, **20**(11) (1972) 1281.

16. TSUBAKINO, H., SODONA, K. & NOZATO, R., *J. Mater. Sci. Lett.*, **12**(3) (1993) 196.